

Compressing Color Computer-Generated Hologram Using Gradient Optimized Quantum-Inspired Neural Network

Jingyuan Ma¹, Guanglin Yang^{1,*}, Haiyan Xie²

¹Laboratory of Signal and Information Processing, School of Electronics, Peking University, Beijing, China

²China Science Patent and Trademark Agent, Beijing, China

Email address:

ygl@pku.edu.cn (Guanglin Yang)

*Corresponding author

To cite this article:

Jingyuan Ma, Guanglin Yang, Haiyan Xie. Compressing Color Computer-Generated Hologram Using Gradient Optimized Quantum-Inspired Neural Network. *American Journal of Optics and Photonics*. Vol. 11, No. 1, 2023, pp. 1-9. doi: 10.11648/j.ajop.20231101.11

Received: August 5, 2023; Accepted: August 28, 2023; Published: September 14, 2023

Abstract: In the existing electronic communication systems, fast transmission of three-dimensional image information requires compression and encoding of holographic images. In this paper, a method for compressing the color computer-generated hologram by the quantum-inspired neural network based on the gradient optimized algorithm is proposed. By optimizing the gradient descent calculation method of quantum-inspired neural network, the convergence speed of the quantum-inspired neural network was improved, and the loss error of the quantum-inspired neural network was reduced. The bandwidth-limited angular spectrum method was used to calculate the color double-phase computer-generated hologram. Gradient optimized quantum-inspired neural networks and traditional quantum-inspired neural networks are used to compress the color double-phase computer-generated hologram respectively, and the decompressed color double-phase computer-generated hologram is reconstructed to the original color image by the angular spectrum method. It is shown that gradient-optimized quantum-inspired neural networks have better results in compressing and reconstructing color computer-generated holograms, which obtain high-quality and low color difference reconstructed original images compared to traditional quantum-inspired neural networks. Different gradient optimization algorithms also have differences in the training of computer-generated holograms at different wavelengths. Therefore, suitable gradient-optimized quantum-inspired neural networks can accelerate the compression speed of computer-generated holograms, while improving the quality of decompressed computer-generated holograms and reconstructed original images.

Keywords: Computer Holography, Image Compression, Neural Network, Quantum Computing, Image Reconstruction

1. Introduction

In computer holography, the computer-generated holograms (CGHs) contain a large amount of information about three-dimensional objects, which includes amplitude and phase information of 3D object. Therefore, to accelerate the transmission of CGHs and achieve the real-time 3D image display, the CGHs should be compressed and fast transmitted. At the same time, the recorded object information in CGHs should not be destroyed during the transmission [1].

In researching, some documents about the digital hologram compression have been investigated, such as in Ref. [2], the back propagation (BP) neural network has been used to

compress CGHs. Researchers have offered a more flexible compression ratio and higher reproduction quality than traditional encoding methods. In Ref. [3], the compression sensing has also been applied to compress CGHs.

Inspired by the principles of quantum computing, the quantum-inspired neural network (QINN) [4, 5] has been used in the field of image processing. The QINN uses the principle of quantum superposition states to provide strong data parallelism. The N-bit qubits can store 2^N -bit information, which expands the understanding and optimization space to enhance the nonlinear ability of the network. In Refs. [6-11], researchers have proved the superior performance of QINN in solving function optimization and image quality restoration. In Ref. [1], the QINN is used to compress the grayscale Fresnel CGHs, and

their method adopted fewer epochs than the BP neural network. In Ref. [12], the initial values of quantum-inspired neural networks are optimized to accelerate the convergence of the network, at the same time it can improve the quality of reconstructed images.

Previously, there have been papers using the quantum-inspired neural network to process the ordinary images and the grayscale CGHs, but this work focuses on the application of QINN to compress and reconstruct the color CGHs. Different from the grayscale CGHs, the data amount of color CGHs is three times that of the grayscale CGHs. It should be ensured that when reconstructing the original object information, each channel has a considerable reconstruction quality to avoid the generation of chromatic aberration. Although QINN has many advantages over ordinary neural networks, it still needs further optimization for QINN itself. The descent algorithm of network gradient determines the speed and convergence effect of model training. Therefore, it is necessary to optimize the stochastic gradient descent (SGD) method to find the most suitable gradient optimization algorithm of QINN.

In this paper, the double-phase CGHs of different wavelengths are obtained by the angular spectrum method (ASM) in the RGB color space [13]. The color CGHs are compressed and reconstructed using optimized QINN. The convergence speed of the network, the quality of decompressed holograms and the quality of reconstructed original color images are evaluated.

2. Band-Limited Double-Phase Computer-Generated Hologram

According to Ref. [14, 15], the bandwidth-limited ASM is adopted in this paper. This method can solve the sampling problem in ASM by limiting the bandwidth and truncating unnecessary high-frequency signals in the input source field, avoiding the aliasing error of the transfer function.

The $u(x, y, z)$ is the complex amplitude distribution of the light field on the observation screen, which can be expressed as the convolution of the complex amplitude distribution $u(x, y, 0)$ of the light field on the back surface of the diffraction screen and the system impulse response $h(x, y, z)$, using the convolution theorem, the formula can be written as

$$U(u, v, z) = F\{u(x, y, 0)\}F\{h(x, y, z)\} = U(u, v, 0)\exp(i2\pi wz), \quad (1)$$

where F represents Fourier transform, u , v and w are Fourier frequencies in x , y and z directions respectively. Therefore, the resulting hologram can be expressed as

$$u(x, y, z) = F^{-1}\{U(u, v, 0)\exp(i2\pi wz)\}. \quad (2)$$

In order to avoid aliasing error, the range of the system function needs to be limited. According to Nyquist theorem, to avoid descent error, the sampling interval should satisfy the following condition

$$|u| \leq u_{limit} = \frac{1}{[(2\Delta uz)^2 + 1]^{1/2} \lambda}, \quad (3)$$

$$|v| \leq v_{limit} = \frac{1}{[(2\Delta vz)^2 + 1]^{1/2} \lambda}. \quad (4)$$

The mathematical expression of the CGH can also be defined as the complex of amplitude $A(x, y)$ and phase $\varphi(x, y)$

$$U(x, y) = A(x, y)e^{i\varphi(x, y)}. \quad (5)$$

The amplitude information of the CGH is encoded into the phase information, which can be expressed as

$$\Phi_1(x, y) = \varphi(x, y) + \cos^{-1}[A(x, y)], \quad (6)$$

$$\Phi_2(x, y) = \varphi(x, y) - \cos^{-1}[A(x, y)], \quad (7)$$

$$U(x, y) = W_1 \exp[i\Phi_1(x, y)] + W_2 \exp[i\Phi_2(x, y)]. \quad (8)$$

where W_1 and W_2 are grating in the shape of complementary checkerboard with the size of $x \times y$, thus a double phase CGH contains both amplitude and phase information of the object light waves [14].

3. Compressing Color CGH with Gradient Optimized QINN

3.1. Quantum-Inspired Neural Network

In quantum computing theory, quantum states expressed in complex numbers can be described as

$$f(\theta) = e^{i\theta} = \cos \theta + i \sin \theta, \quad (9)$$

where θ is the phase of the quantum state, and the values of the real part and imaginary part correspond to the probability amplitudes of $|0\rangle$ and $|1\rangle$ respectively.

The quantum-inspired neural network is composed of quantum neurons. The computational process of quantum neurons [1] is as follows

$$u = \sum_{i=1}^L f(\theta_i) f(I_i) - f(\lambda), \quad (10)$$

$$y = \frac{\pi}{2} g(\delta) - \arg(u), \quad (11)$$

$$O = f(y), \quad (12)$$

where $g(x) = 1/[1 + \exp(-x)]$, $\arg(\cdot)$ represents the phase of the complex number, L is the number of input quantum neuron, O represents the output of the quantum neuron, the phase parameter θ and the threshold λ corresponds to the one-bit rotation gate, and the reversal parameter δ corresponds to the two-bit CNOT gate.

The input data of the quantum-inspired neural network needs to be normalized to $[0, 1]$ and then converted to the phase range $[0, \pi/2]$ of the quantum state. The data of the input layer can be expressed as

$$I_l = \frac{\pi}{2} \text{input}_l. \quad (13)$$

The output value of the n th quantum neuron in the last layer is expressed as the probability of $|1\rangle$.

$$\text{output}_n = |\text{Im}(O_n)|^2, \quad (14)$$

$$\text{Err} = \frac{1}{2} \sum_{b=1}^B \sum_{n=1}^N (\text{target}_{n,b} - \text{output}_{n,b})^2, \quad (15)$$

where B is the number of sub image blocks, N is the number of neurons, $\text{target}_{n,b}$ and $\text{output}_{n,b}$ are the target output value and the actual output value of the n th layer neural network.

3.2. Quantum-Inspired Neural Network with Gradient Descent Optimization Algorithms

In SGD algorithms, a larger learning rate causes the QINN gradient to decrease quickly but may miss the maximum point of the loss function. However, a smaller learning rate will make the QINN converge slowly. Therefore, several experiments are needed to choose an appropriate learning rate. At the same learning rate, the threshold parameters of all quantum gates are updated synchronously, but depending on different data characteristics, different gradient update magnitudes may be required, which cannot be achieved by SGD. In addition, a key issue of SGD training is whether the network is trapped in the saddle point and cannot escape, thus it cannot reach the minimum point of the error function.

In the backpropagation process of quantum-inspired neural network, the update of quantum neuron parameters can be expressed as

$$\theta^n = \theta^{n-1} - \eta \frac{\partial E}{\partial \theta^{n-1}}, \quad (16)$$

$$\lambda^n = \lambda^{n-1} - \eta \frac{\partial E}{\partial \lambda^{n-1}}, \quad (17)$$

$$\delta^n = \delta^{n-1} - \eta \frac{\partial E}{\partial \delta^{n-1}}, \quad (18)$$

where η is the learning rate.

In this paper, Momentum, Adagrad, Adadelata, and Adam algorithm [16, 17] are used to analyze the gradient descent problem of QINN. The parameter θ of the phase-shifted quantum gate $R(\theta)$ is used as an example to introduce its update, and the parameters γ and δ of the controlled non-gate $U(\gamma)$ are updated in the same way as θ .

The Momentum is an optimization algorithm that suppresses the gradient oscillation and can accelerate the

gradient descent in the relevant direction of the neural network. The three parameters can be updated according to the following rules. The γ is usually set to 0.9, the v represents the exponential weighted average of the gradient.

$$v_t = \gamma v_{t-1} + \eta g_t, \quad (19)$$

$$\theta_{t+1} = \theta_t - v_t. \quad (20)$$

The Adagrad can adjust the learning rate according to the quantum spin gate parameters adaptively. It doesn't require manual setting of the learning rate, and the $\eta=0.01$ is adopted in most tasks. The historical gradient information is considered in the process of new gradient updating, the G_t is the squares sum of historical gradients, the ε is the smoothing factor, and the value is e^{-8} .

$$\theta_{t+1} = \theta_t - \frac{\eta}{\sqrt{G_t + \varepsilon}} g_t. \quad (21)$$

The Adadelata is used to reduce the learning rate of monotonic descent in the Adagrad. The Adadelata limits the accumulation window of past gradients to a fixed size, instead of accumulating all past squared gradients. The moving average of the gradients at each moment depends only on the average gradient value of the previous moment and the current gradient value. E is mathematic expectation.

$$E[g^2]_t = \gamma E[g^2]_{t-1} + (1-\gamma)g_t^2, \quad (22)$$

$$\Delta \theta_t = -\frac{\eta}{E[g^2]_t + \varepsilon} g_t, \quad (23)$$

$$\theta_{t+1} = \theta_t - \Delta \theta_t, \quad (24)$$

The Adam is another algorithm to calculate the adaptive learning rate for each parameter. In order to store the moving average of the squared gradient, the Adam algorithm also maintains the exponential decay average of the previous and present gradients. It is essentially the Adadelata algorithm with momentum term, and after bias correction, the effective learning rate of each step changes within a certain range.

$$m_t = \beta_1 m_{t-1} + (1-\beta_1)g_t, \quad (25)$$

$$v_t = \beta_2 m_{t-1} + (1-\beta_2)g_t^2, \quad (26)$$

The m_t and v_t are the biased first-order moment estimates of the gradient and the biased second-order moment estimates of the gradient, respectively. The β_1 and β_2 are the exponential decay rates of the first-order moment estimates and second-order moment estimates of the gradient, respectively, the value range is controlled in $[0, 1]$. To control the range of variation of the learning rate, the bias is updated for the gradient first-order moment estimates and second-order moment estimates as

$$\hat{m}_t = \frac{m_t}{1 - \beta_1^t} \quad (27)$$

$$\hat{v}_t = \frac{v_t}{1 - \beta_2^t}, \quad (28)$$

$$\theta_{t+1} = \theta_t - \frac{\eta}{\sqrt{\hat{v}_t + \epsilon}} \hat{m}_t. \quad (29)$$

3.3. Compressing Color Computer-Generated Hologram

A three-layer QINN structure [18-20] is constructed to compress color CGHs. The number of hidden neurons (e. g., K) is smaller than the number of input neurons (e. g., L), and the

number of input neurons is equal to the number of output neurons. The color CGH is compressed from the input layer to the hidden layer, and the color CGH is decompressed from the hidden layer to the output layer. The output data of the hidden layer is the compressed color CGH, and the output data of the output layer is the decompressed color CGH.

First, the double-phase color CGH is computed in RGB space. In the data preprocessing stage, the color CGHs are extracted into three RGB channels. The CGHs (e. g., $X \times Y$ pixels) are normalized from $[0, 255]$ to $[0, 1]$, and divided into sub-image blocks (e. g., $x \times y$ pixels, $B = (X \times Y) / (x \times y)$). Then the sub-image blocks are transformed into column vectors (e. g., $L \times 1 = x \times y$) as the final network input.

The process of compressing a color CGH by the QINN can be represented in Figure 1.

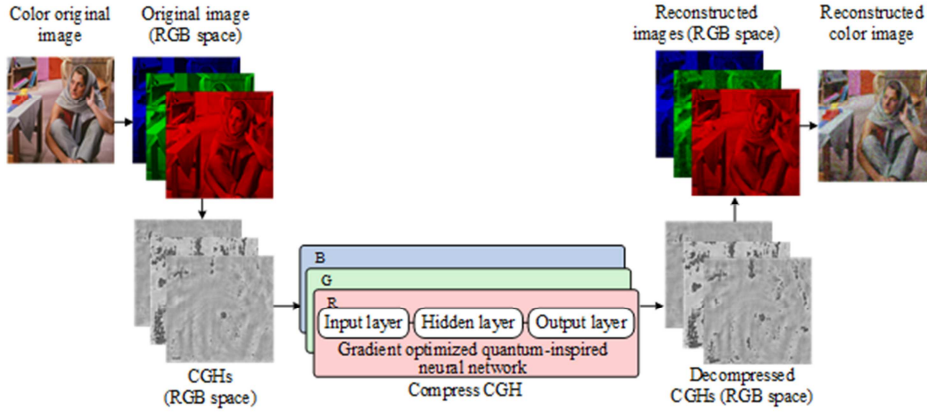


Figure 1. Color CGH compression using QINN based on RGB channels.

4. Experiment and Analysis

4.1. Calculation and Reconstruction of Color Computer-Generated Hologram

The authors of Ref. [1] used quantum-inspired neural networks to compress a single grayscale Fresnel hologram. And it is experimentally demonstrated that quantum-inspired neural networks converge to the expected loss value faster compared to traditional bp neural networks, and also obtain higher PSNR of the reconstructed image. A three-channel quantum-inspired neural network structure for compressing color computer holograms is proposed, and extends the compression method from a single image to a training set to enhance the network's generalization ability.

The specific approach of the experiments in this paper is to divide the holograms of each color channel of RGB into a dataset separately, and train different three network models in different channels to obtain different quantum neural nets, each of which is able to learn the features of the corresponding color hologram. The advantage of this approach is that each quantum-inspired neural network model learns the features of the dataset more uniformly and can obtain different compression models for each color channel hologram, which can produce higher quality decompressed color CGHs.

The calculation conditions of color CGHs calculated by ASM are as follows: the wavelengths of red, green and blue

are 633, 532 and 450 nm, respectively, the size of the original image is 256×256 pixels, the size of hologram is 256×256 pixels, and the distance between the color original image and the CGH is 0.3m. The pixel sizes corresponding to the RGB channels are 21×10^{-3} mm, 19×10^{-3} mm and 17×10^{-3} mm, respectively.

4.2. Quality Evaluation Index

The indexes to evaluate the effect of network compression include holographic image compression rate (CR) and loss reduction speed. The indexes to evaluate the quality of compressed CGHs and reconstructed CGHs are the mean square error (MSE), the peak-signal-to-noise ratio (PSNR), and the structural similarity index measure (SSIM).

$$CR = \frac{S_c}{S_0} = \frac{K}{L}, \quad (30)$$

$$MSE = \frac{1}{X \times Y} \sum_{x=1}^X \sum_{y=1}^Y |f(x, y) - \bar{f}(x, y)|^2, \quad (31)$$

$$PSNR = 10 \log_{10} \frac{x^2}{MSE}, \quad (32)$$

where the S_c and S_0 represent the size of the compressed CGH and the original CGH. The $f(x, y)$ and $\bar{f}(x, y)$

represent the reconstructed CGH and the original CGH. the x is the peak-to-peak value of the CGH data.

$$\text{SSIM}(x, y) = l(x, y)^\alpha \cdot c(x, y)^\beta \cdot s(x, y)^\gamma$$

$$= \frac{(2u_x u_y + c_1)(2\sigma_{xy} + c_2)}{(u_x^2 + u_y^2 + c_1)(\sigma_x^2 + \sigma_y^2 + c_2)} \quad (33)$$

where the $l(x, y)$, $c(x, y)$, and $s(x, y)$ are the image brightness, contrast and structure contrast functions respectively, the σ_x^2 is the variance of x , the σ_y^2 is the variance of y , the σ_{xy} is the covariance of x and y . The c_1 , c_2 , and c_3 are set to constants. The SSIM is a number between 0 and 1. The larger SSIM means less difference between the two images and better image quality.

4.3. Compressing Color Computer-Generated Hologram with Quantum-Inspired Neural Network

The color CGHs are divided into three channels of RGB, and the color CGHs are compressed and decompressed in each channel. The QINN is initialized with a randomly generated threshold. The CSIQ dataset [21] is computed as double-phase

CGHs, and then 20 CGHs are selected as the training set for QINN. The input CGH size is unified to 256×256 pixels, then divided into sub-image blocks with pixel size of 8×8 , and the final input data size is 64×1 . Therefore, the number of quantum neurons in the input and output layers is 64, and the number of quantum neurons in the hidden layer is set to 32, 16, 8 and 4, respectively. The image compression ratios corresponding to the four network structures are 0.5, 0.25, 0.125, and 0.0625. Barbara image is used for test image.

Table 1 shows the loss values of network convergence MSE, PSNR, and SSIM of the decompressed CGH for different compression ratios. Comparing the image quality of each channel, it can be concluded that the PSNR and SSIM of the decompressed CGH decrease as the CR decreases. When the compression ratio is 0.5, the PSNRs of the three RGB channels are the highest. Comparing different color channels, it can be found that PSNR and SSIM of the decompressed red light CGHs are highest, and those of green light CGHs are lowest. The reason for this phenomenon is the difference in pixel values and distributions of different color wavelengths CGHs, which lead to differences in network training and reconstructed image quality.

Table 1. MSE, PSNR and SSIM of decompressed CGHs with different compression ratios.

| CR | R | | | G | | | B | | |
|--------|----------|---------|--------|----------|---------|--------|----------|---------|--------|
| | MSE | PSNR | SSIM | MSE | PSNR | SSIM | MSE | PSNR | SSIM |
| 0.500 | 0.000954 | 35.1833 | 0.9955 | 0.001298 | 29.5024 | 0.9907 | 0.000920 | 29.5325 | 0.9900 |
| 0.250 | 0.002069 | 30.4329 | 0.9858 | 0.005268 | 20.3886 | 0.9331 | 0.002677 | 28.1127 | 0.8990 |
| 0.125 | 0.003410 | 29.2379 | 0.9832 | 0.009542 | 17.1336 | 0.8553 | 0.004461 | 25.4032 | 0.8936 |
| 0.0625 | 0.004251 | 28.4368 | 0.9825 | 0.013076 | 15.6008 | 0.7792 | 0.005649 | 24.2012 | 0.8879 |

Table 2 lists the PSNR and SSIM of the reconstructed original image from the decompressed CGH for different channels and compression ratios. It can be noticed that the index value of each reconstructed image is lower than that of the decompressed CGH due to the introduction of image noise

during the reconstruction of the CGH. However, the index value of each reconstructed image is positively correlated with the index value of the decompressed CGH. The quality of the reconstructed original images is also highest when CR is 0.5.

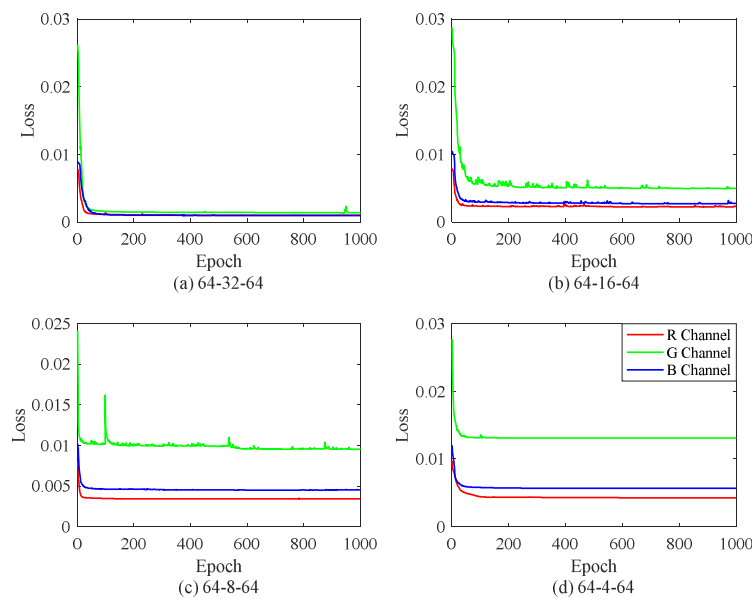


Figure 2. The variation of training loss with the increment of training epochs.

Table 2. PSNR and SSIM of reconstructed image with different compression ratios.

| CR | R | | G | | B | |
|--------|---------|--------|---------|--------|---------|--------|
| | PSNR | SSIM | PSNR | SSIM | PSNR | SSIM |
| 0.500 | 27.6237 | 0.6152 | 25.5007 | 0.4070 | 25.4957 | 0.4270 |
| 0.250 | 25.3070 | 0.4867 | 19.3357 | 0.1323 | 22.1881 | 0.3398 |
| 0.125 | 23.9600 | 0.3705 | 18.2079 | 0.0741 | 20.8981 | 0.2344 |
| 0.0625 | 23.2320 | 0.3182 | 17.3656 | 0.0518 | 20.3307 | 0.2369 |

Figure 2 shows the curves of loss reduction in different channels. Figure 3 shows the decompressed CGHs and the reconstructed original images in the three channels. The pixel distribution of CGHs in different color channels varies greatly, among which the pixel distribution of green light holograms is more complex, which leads to different decreasing speed of loss values and different convergence to different error values

in different color channels. When the compression ratio of the network decreases, the ability of the network to characterize the pixel distribution decreases in the same network structure, and the more complex the pixel distribution of the training set has a greater impact on the network performance. Therefore, the green and blue channel loss curves converge to a larger error and their reconstructed image quality is lower.

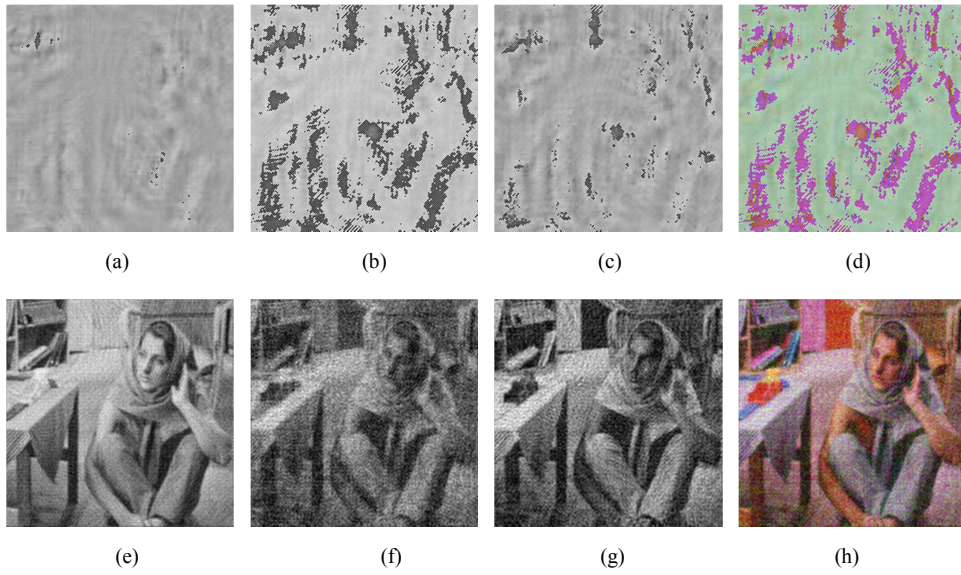


Figure 3 (a), (b), (c) corresponding to decompressed CGHs in RGB channels, respectively. (d) Color CGH. (e), (f), (g) corresponding to reconstructed image in RGB channels, respectively. (h) Color reconstructed image.

4.4. Compressing Color Computer-Generated Hologram with Gradient Optimized Quantum-Inspired Neural Network

Different gradient optimization algorithms will bring

different gradient convergence rates and eventually converge to different loss values. Gradient descent curves of different gradient optimization algorithms in RGB channel can be represented by Figure 4.

Table 3. MSE, PSNR and SSIM of decompressed CGHs with different optimization algorithm.

| | R channel | | | G channel | | | B channel | | |
|-----------|-----------|---------|--------|-----------|---------|--------|-----------|---------|--------|
| | MSE | PSNR | SSIM | MSE | PSNR | SSIM | MSE | PSNR | SSIM |
| SGD | 0.000954 | 35.1833 | 0.9955 | 0.001298 | 29.5024 | 0.9907 | 0.000920 | 29.5325 | 0.9900 |
| Momentum | 0.000954 | 35.0164 | 0.9952 | 0.001361 | 28.9773 | 0.9890 | 0.001343 | 29.4289 | 0.9891 |
| Adagrad | 0.001038 | 34.8187 | 0.9953 | 0.002575 | 28.6245 | 0.9900 | 0.001221 | 29.2733 | 0.9898 |
| Adadelata | 0.001203 | 35.3599 | 0.9959 | 0.001625 | 22.1372 | 0.9579 | 0.001483 | 28.0256 | 0.9864 |
| Adam | 0.000940 | 36.0076 | 0.9963 | 0.001370 | 29.6871 | 0.9914 | 0.001109 | 29.7076 | 0.9905 |

Table 3 shows that when $CR = 0.5$ different gradient optimization algorithms are used to compare the image quality evaluation indexes of holograms decompressed by each channel. The loss value of Adam algorithm is the lowest, and the PSNR and SSIM values are the highest. Compared among

the three channels, the quality of decompressed CGHs in R channel is the highest.

Table 4 shows the PSNR and SSIM of the reconstructed original image of different gradient optimization algorithms corresponding to different color channels when $CR = 0.5$. In

each channel, the reconstructed image quality of Adam's method is the best. The PSNR values of each gradient

optimization algorithm in the R channel are better than those of the SGD algorithm.

Table 4. PSNR of reconstructed image with different optimization algorithm.

| | R | | G | | B | |
|-----------|---------|--------|---------|--------|---------|--------|
| | PSNR | SSIM | PSNR | SSIM | PSNR | SSIM |
| SGD | 27.6237 | 0.6152 | 25.5007 | 0.4070 | 25.4957 | 0.4270 |
| Momentum | 27.7827 | 0.6326 | 25.2601 | 0.3946 | 25.6201 | 0.4371 |
| Adagrad | 27.8068 | 0.5992 | 24.4479 | 0.3657 | 25.6353 | 0.4381 |
| Adadelata | 28.2016 | 0.6217 | 21.3977 | 0.2262 | 24.6048 | 0.3870 |
| Adam | 28.2357 | 0.6595 | 25.7401 | 0.4209 | 25.8083 | 0.4586 |

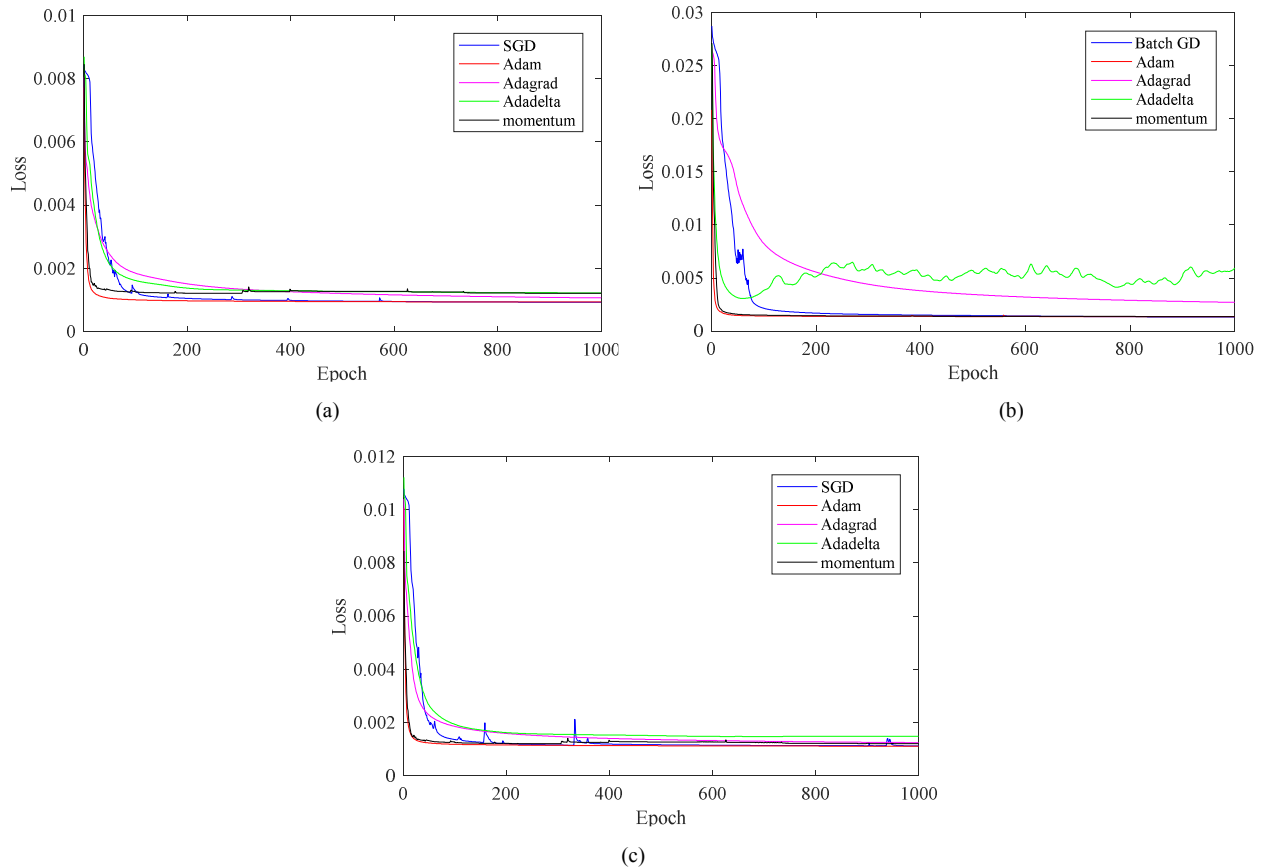


Figure 4. Gradient descent curves of different gradient optimization algorithms in R, G, and B channel.

It can be seen from Figure 4, the red curve is the Adam optimization algorithm with the fastest gradient descent and the best convergence. The convergence error value of SGD is similar to that of Adam, but its convergence speed is the slowest. The convergence speed of the momentum algorithm

is similar to that of the Adam algorithm, but the final convergence error value is larger than that of the Adam algorithm. The convergence speed of Adagrad and Adadelata are similar and both are faster than the SGD algorithm, but the final convergence error value of Adadelata is poor.



(a) Original reconstructed image



(b) SGD



(c) Momentum



Figure 5. Reconstructed image of different optimized algorithm.

From the perspective of human visual observation, the reconstructed images of Adam algorithm and Momentum algorithm have higher clarity, among which the reconstructed image color based on Adam algorithm is closer to Figure 5. (a), and the color difference is smaller than that of Momentum algorithm, and the reconstructed image noise of Momentum algorithm is more than that of Adam algorithm. The reconstructed original image colors of Adagrad, Adadelata, and SGD algorithms are similar, and the reconstructed images are more violet than the remaining two algorithms, which is consistent with the numerical results of the indexes in Table 4. The reconstructed image of the green CGH is noisier, and its noise distribution is different from that of the reconstructed images of the red CGH and the blue CGH, thus leading to the fusion of the red and blue channel noise to form the purple color, while the green channel noise is not fused and thus presented in the final color reconstructed image.

5. Conclusion

In this paper, a gradient optimized QINN algorithm for compressing color CGH in RGB space is proposed. In the RGB color space, the bandwidth limited angular spectrum method is used to calculate the double phase hologram by computer. Because this method uses a real value CGH to record the phase and amplitude information of the spatial complex function, without introducing additional bias terms, it reduces the introduction of noise during the reconstruction process. Therefore, it can achieve higher image quality and smaller color difference in the reconstruction process of decompressed color CGH. Four different QINN gradient optimization algorithms were proposed in the compression algorithm. The experimental results show that the gradient optimized QINN has faster convergence speed, lower convergence error, and higher quality reconstructed original color images. When $CR=0.5$, the reconstructed color images decompressed by the QINN network using the Adam algorithm have a PSNR improvement of 0.388dB and a SSIM improvement of 0.03 compared to traditional QINN. Therefore, compared to traditional QINN, utilizing different gradient optimization algorithms has great potential.

Acknowledgements

The authors would like to thank the Spatial Image Processing Laboratory for their support. This work was supported by the National Natural Science Foundation of China (No. 62071009).

References

- [1] M. Liu, G. Yang, and H. Xie, "Method of computer-generated hologram compression and transmission using quantum back-propagation neural network," *Opt. Eng.* 56(2), 023104 (2017).
- [2] C. Zhang, G. Yang, and H. Xie, "Information compression of computer-generated hologram using BP neural network," in *Biomedical Optics and 3-D Imaging*, OSA Technical Digest (2010), paper JMA2.
- [3] Y. Sun, G. Yang, and H. Xie, "Computer-generated hologram fast transmission using compressive sensing," in *2016 Imaging and Applied Optics*, OSA Technical Digest (2016), paper JW4A.
- [4] S. K. Jeswal and S. Chakraverty, "Recent Developments and Applications in Quantum Neural Network: A Review," *Arch. Comput. Methods Eng.* 26(4), 793–807 (2019).
- [5] Z. A. Jia, B. Yi, R. Zhai, Y. C. Wu, G. C. Guo, and G. P. Guo, "Quantum Neural Network States: A Brief Review of Methods and Applications," *Adv. Quantum Technol.* 2(7–8), 1–16 (2019).
- [6] D. Konar, S. Bhattacharyya, T. K. Gandhi, and B. K. Panigrahi, "A Quantum-Inspired Self-Supervised Network model for automatic segmentation of brain MR images," *Appl. Soft Comput. J.* 93, 106348 (2020).
- [7] K. Mori, T. Isokawa, N. Kouda, N. Matsui, and H. Nishimura, "Qubit inspired neural network towards its practical applications," in *the 2006 IEEE International Joint Conference on Neural Network Proceedings* (2006), pp. 224–229.
- [8] L. S. Panchi, "Learning algorithm and application of quantum BP neural networks based on universal quantum gates," *J. Syst. Eng. Electron.* 19(1), 167–174 (2008).
- [9] C. Wang and J. H. Du, "Research of Image Compression Based on Quantum BP," *Dianzi Yu Xinxu Xuebao/Journal Electron. Inf. Technol.* 28(5), 848–851 (2006).

- [10] M. Cao, "Quantum-inspired Neural Networks with Applications," *Int. J. Comput. Inf. Technol.* 03(01), 83–92 (2014).
- [11] X. F. Niu and W. P. Ma, "Design of a novel quantum neural network," *Laser Phys. Lett.* 17(10), (2020).
- [12] S. Hou, G. Yang, and H. Xie, "Optimized initial weight in quantum-inspired neural network for compressing computer-generated holograms," *Opt. Eng.* 58(05), 053105 (2019).
- [13] K. Matsushima and T. Shimobaba, "Band-limited angular spectrum method for numerical simulation of free-space propagation in far and near fields," *Opt. Express* 17(22), 19662-19673 (2009).
- [14] Y. K. Kim, J. S. Lee, and Y. H. Won, "Low-noise high-efficiency double-phase hologram by multiplying a weight factor," *Opt. Lett.* 44(15), 3649-3652 (2019).
- [15] V. Arrizón and D. Sánchez-de-la-Llave, "Double-phase holograms implemented with phase-only spatial light modulators: performance evaluation and improvement," *Appl. Opt.* 41(17), 3436 (2002).
- [16] S. Ruder, "An overview of gradient descent optimization algorithms," *arXiv.1609.04747* (2016).
- [17] D. K. R. Gaddam, M. D. Ansari, S. Vuppala, V. K. Gunjan, and M. M. Sati, "A Performance Comparison of Optimization Algorithms on a Generated Dataset," *Lect. Notes Electr. Eng.* 783 (January), 1407–1415 (2022).
- [18] T. Shimobaba, M. Makowski, Y. Nagahama, Y. Endo, R. Hirayama, D. Hiyama, S. Hasegawa, M. Sano, T. Kakue, M. Oikawa, T. Sugie, N. Takada, and T. Ito, "Color computer-generated hologram generation using the random phase-free method and color space conversion," *Appl. Opt.* 55 (15), 4159-4165 (2016).
- [19] T. Shimobaba, T. Kakue, and M. Oikawa, et al. "Calculation reduction method for color digital holography and computer-generated hologram using color space conversion," *Opt. Eng.* 53(2) 024108 (2014).
- [20] H. Nakayama, N. Takada, Y. Ichihashi, S. Awazu, T. Shimobaba, N. Masuda, and T. Ito, "Real-time color electroholography using multiple graphics processing units and multiple high-definition liquid-crystal display panels," *Appl. Opt.* 49(31), 5993–5996 (2010).
- [21] E. C. Larson and D. M. Chandler, "Most Apparent Distortion: A Dual Strategy for Full-Reference Image Quality Assessment," *Image Qual. Syst. Perform.* VI, 7242 (2009), paper 72420S.